UCLA
Technical Reports

Title

High Resolution River Hydraulic and Water Quality Characterization Using Rapidly Deployable Networked Infomechanical Systems (NIMS RD)

Permalink

https://escholarship.org/uc/item/5pt8v7b2

Authors

Thomas C. Harmon
Richard F. Ambrose
Robert M. Gilbert
et al.

Publication Date

2006

High Resolution River Hydraulic and Water Quality Characterization Using Rapidly Deployable Networked Infomechanical Systems (NIMS RD)

Thomas C. Harmon[1*], Richard F. Ambrose[2], Robert M. Gilbert[3], Jason C. Fisher[1], Michael Stealey[4], and William J. Kaiser[4]

Center for Embedded Networked Sensing (CENS)

Technical Report No. 60

February 1, 2006

*corresponding author: email – tharmon@ucmerced.edu, phone: (209) 724-4337

[1] School of Engineering, PO Box 2039, University of California, Merced, CA 95340.

[2] Environmental Science & Engineering Program and Department of Environmental Health Sciences, Box 951772, University of California, Los Angeles, CA 90095-1772.

[3] Department of Environmental Health Sciences, Box 951772, University of California, Los Angeles, CA 90095-1772.

[4] Electrical Engineering Department, Box 951594, University of California, Los Angeles, CA 90095-1594.

High Resolution River Hydraulic and Water Quality Characterization Using Rapidly

Deployable Networked Infomechanical Systems (NIMS RD)

Abstract

Increasing demands on water supplies, non-point source pollution, and water quality-based ecological concerns all point to the need for observing stream flow perturbations and pollutant discharges at higher resolution than was practical in the past. This work presents a rapidly deployable Networked Infomechanical System (NIMS RD) technology for observing spatiotemporal hydraulic and chemical properties across stream channels. NIMS RD is comprised of two supporting towers and a suspension cable delivering power and Internet connectivity for controlling and actuating the tram-like NIMS unit. The NIMS unit is capable of raising and lowering a payload of sensors, allowing a preprogrammed or data-actuated adaptive scan to be completed across a stream channel. In this work, NIMS RD is demonstrated in two relevant cases: (1) elucidating spatiotemporal variations in nutrients and other biologically significant stream constituents in Medea Creek, a small urban stream in Southern California, and (2) using high resolution synoptic sampling of steady velocity and salinity distributions across the San Joaquin River in Central California to provide quantitative salt load estimates. For Medea Creek, temperature and specific conductivity (SC) exhibited varying cross-sectional patterns throughout each of three 24-hour scans carried out over three summer months. Both temperature and SC displayed repeating sinusoidal diel fluctuations independent of the spatial variation. For each of the months the cross-sectional variation was lower during the

late nighttime and morning hours than during the afternoon and early nighttime hours. For the San Joaquin River, high resolution velocity distributions from NIMS RD were successfully reproduced in separate deployments, and quantitatively matched stage-based volumetric flow rates at the site. The product of the velocity and associated SC distributions yielded total salt load estimates similar to report values, but no basis for direct comparison was available.

1. Introduction

This paper introduces a rapidly deployable Networked Infomechanical Systems (NIMS RD) technology that facilitates the study of flow and water quality in rivers and streams. Degraded river water quality is the norm in the world's populated and agricultural regions due to the impacts of point and non-point source pollution (Laroche *et al*., 1996; Walsh *et al*., 2005). In arid and semi-arid regions, degradation may be exacerbated by reduced dilution caused by upstream water impoundments or withdrawals. Restoring and maintaining river quality in human-dominated regions requires striking a balance between river water quality and water supply demands, wastewater disposal needs, groundwater accretions, agricultural drainage flows and urban runoff. Given the distributed nature of the properties of rivers and their inputs, a major challenge then arises in observing or monitoring water quality changes with sufficient resolution to link those changes to specific events (e.g., reservoir releases) or land management practices (e.g., fertilization). Without a clear link, it is difficult to identify a rational strategy for assigning water quality management objectives.

On a regional or basin scale, using traditional (sparse) gauging station data to calibrate one-dimensional flow and mixing models is a useful approach for estimating downstream flows and water quality based on upstream releases, withdrawals and returns. For example, this simplistic approach is currently used to manage one of the largest water conveyance systems in the world in Central California (CDWR 2003). On sub-basin or smaller scales, spatiotemporal variability of velocity and water quality properties result from pollutant inputs, hydrodynamic mixing regimes, and the biogeochemical cycling processes that are themselves distributed in time and space. Higher resolution observations are needed if we are to understand processes well enough to predict conditions and manage water quality at these scales (e.g., Quinn et al., 2005).

A variety of remote-controlled and autonomous systems exist for transporting velocity and water quality sensors through aquatic systems. Buoyed or moored deployment platforms provide vertical profiling capabilities over long time periods at key locations (Honji *et al.*, 1987; Luettich, 1993; Doherty *et al.*, 1999; Reynolds-Fleming *et al.*, 2002). Autonomous underwater vehicles (AUVs) have been used extensively by the oceanographic community, and more recently in lakes and river systems. These robotic devices can be programmed to follow prescribed courses (Laval *et al.*, 2000; Yu *et al.*, 2002) or to sample adaptively, for example, to track a contaminant plume (Bachmayer *et al.*, 2004; Ogren *et al.*, 2004; Farrell *et al.*, 2005). These efforts can lead to important insights into flow and water quality spatiotemporal distributions within a reach of 10s to 100s of meters with a quarterly frequency. However, one can also envision posing hypotheses for which testing demands a still greater spatiotemporal sampling granularity, on the order cm to m spatially and minutes to hours in frequency.

The purpose of this paper is to introduce a new technology for obtaining high resolution observations of spatiotemporal river channel hydraulic and water quality patterns. NIMS RD is an example of the distributed embedded networked sensing and actuation technology that has developed over the last decade to enable the vision of pervasive observation of the environment. NIMS employs an infrastructure-supported mobility that enables sensor nodes to explore and characterized complex, three-dimensional environments. This paper describes the NIMS RD device hardware, software, and deployment technique, then demonstrates the technology by mapping the river cross-sectional temperature and salinity at a location on Medea Creek in Southern California, and by mapping velocity and salinity on a San Joaquin River channel cross-section in Central California.

2. NIMS RD System

Networked Infomechanical Systems (NIMS) is a broad new research thrust directed to fundamental advances in the ability to monitor and ultimately control environments through distributed sensing and actuation. NIMS introduces a new form of infrastructure-supported mobility that enables sensor nodes to explore and characterize complex, three-dimensional environments. NIMS enables precise, low energy and sustainable motion with an elevated and adjustable perspective. NIMS cableway systems are readily attached to available or installed infrastructure at a cost similar to that of fixed node installation. The availability of infrastructure allows large mass sensor payloads to be manipulated with low energy actuation. Also, NIMS algorithms permit continuous and autonomous control of node position to adapt to characteristically unpredictable environmental events.

5

The NIMS Rapidly Deployable (NIMS RD) system, shown in Figure 1, is an architecture that scales from compact to large scanning range. NIMS RD systems including complex sensor payloads may be deployed with small personnel teams in a time of one to several hours. The NIMS system includes an embedded computing platform providing control to motor systems that actuate the NIMS cable systems for horizontal and vertical transport, as shown in Figure 1. NIMS software systems then proceed, autonomously and in an unattended fashion, to scan sensor nodes through the environment according to either regular sampling patterns or in-field adaptive patterns. Wireless interfaces provide access to user interfaces (via notebook or handheld PDA devices).

3. Demonstration Site Selection Rationale and Characterization

NIMS RD was deployed at a small creek and a moderately large river to test its performance over a wide range of physical conditions. The first deployment was carried out at Medea Creek in Los Angeles County, CA, a small headwater stream in the Malibu Creek Watershed (Figure 2a). Deploying at Medea Creek provided an opportunity to observe high-resolution stream constituent dynamics in a sub-watershed where the constituent levels are of great public concern due to the level of urbanization occurring in the Malibu Creek Watershed. Medea Creek is listed for algae impairment under Section 303(d) of the Clean Water Act. To reduce the algal biomass, the US Environmental Protection Agency is in the process of decreasing the Total Maximum Daily Loads for nutrients in Malibu Creek. In addition to the research and regulatory interests, the site also provided an opportunity to tackle challenges of deploying in densely vegetated and steeply sloped riparian environments.

The second deployment was executed over a 55m span across the San Joaquin River, just below its confluence with the Merced River (Figure 2b). This site was selected because it provided a challenge for the NIMS RD at a larger scale, and because it afforded an opportunity to develop detailed observations of the hydrodynamic mixing in the confluence zone. Flow in the San Joaquin River is dominated by agricultural and managed wetland drainage in the late fall. Its flow tends to diminish while increasing in temperature and salinity at this time of the year. The Merced River, in contrast, is relatively cold and less saline as it enters San Joaquin. The two rivers had comparable flows at the time of the deployment (October 6-7, 2005), resulting in a visually distinct mixing zone roughly midway across the confluence zone.

In both deployments, the NIMS RD carried a multi-parameter water quality sonde (Hach Environmental, MiniSonde 4a) equipped with temperature, conductivity (specific conductance, SC), nitrate, ammonium and pH sensors. For the San Joaquin River deployment an acoustic Doppler velocity sensor (Sontek Triton ADV) was also suspended from the NIMS RD unit at the same level and just upstream of the water quality sonde. This work focuses on the temperature and SC for the Medea Creek deployment, and on velocity and SC for the San Joaquin River. The temperature sensor in the MiniSonde was a stainless steel variable resistance thermistor (accuracy $\pm$ 0.1 °C; resolution 0.01 °C). The SC sensor was an open-cell graphite electrode design with a working range of 0 to 100 μS/cm (accuracy $\pm$ 0.5% measured value; resolution 0.001 μS/cm). The velocity sensor has a working range of 0.001 to 6 m/s (accuracy $\pm$ the greater of 0.1% measured value or 1 mm/s; resolution 0.1 mm/s).

7

The NIMS RD delivers sensors to depths below the water surface using a predetermined sampling grid or adaptive sampling algorithms. Regular sampling grids were employed in both deployments. For Medea Creek, the sample grid was determined *in situ* at the beginning of each deployment. A plumb line was used to determine the sample points. The plumb line was shuttled across the stream at 20 cm intervals from bank to bank. At each interval the distance from the water line to the creek bottom was determined. Sample points were assigned every 20 cm for each of the vertical transects. The resulting 20 cm by 20 cm grid, comprised of 64 points, required 25 minutes for each scan. For the San Joaquin River deployment, a kayak-based echo-sounder operating at 210 kHz (Valeport, Midas Surveyor) was used to employ a relatively sparse and fine sampling grid in order to test the effects of sampling density. The sparse sampling was executed on a regular 18 cm horizontal by 5 cm vertical spatial intervals (total 53 points) and required approximately 42 min to complete. Sample spacing for the fine grid was 6 cm by 2 cm (309 total points) and required 3 h 20 min to scan.

All the sensors utilized internal logging for data collection. Similarly, the scripts controlling the NIMS-RD motors wrote time-stamped (x, z) sample coordinates to a log file after every move. Before each deployment, the internal clocks for all sensors deployed were synchronized with the notebook computer that actuated the motor system. Using the time stamp as a common variable between data sets, the (x, z) position log file was combined with the sensors' log files.

To examine cross-sectional patterns, contour plots were constructed from interpolated data points. Interpolation of the Medea Creek data was performed using a gridded bivariate interpolation method, based on an algorithm from Akima (1978) and using a

uniform spatial grid for the interpolated data with 0.2 cm resolution. The spatial domain for the Medea Creek contour plots is the convex hull determined by the sampling locations. The gridded bivariate interpolation method was also applied to the San Joaquin River ADV velocity data, but a zero-velocity boundary was assumed at the bathymetric surface. For the specific conductivity (SC) data, interpolation was implemented with an inverse distance weighted interpolation method (inverse distance weighting power of 3). The spatial grid for the San Joaquin River interpolated data has a 2 cm resolution. In this case, the spatial domain for the contour plots was defined by the bathymetry within the cross-section and the elevation of the water surface. The volumetric flow rate, Q, was calculated using the interpolated velocity distribution as

$$Q = \sum_{i=1}^{N} \begin{cases} A_i V_i & \text{for i in } \Omega, \\ 0 & \text{otherwise.} \end{cases} \qquad (1)$$

where N is the total number of grid elements, A_i is the area of element i, V_i, is the water velocity of element i, and Ω is the spatial domain of the cross-section. Similarly, the TDS flux or load, F, is calculated as

$$F = \sum_{i=1}^{N} \begin{cases} 0.65(SC_i) A_i V_i & \text{for i in } \Omega, \\ 0 & \text{otherwise.} \end{cases} \qquad (2)$$

where SC_i is the Specific Conductivity of element i, and 0.65 is a conversion factor (μS/cm to mg/L TDS).

4. Results and Discussion

For visualizations and analysis, each scan is considered a discrete point in time. This assumption requires relatively short scan durations, and constant flow and transport conditions over the course of the scan. For the high resolution San Joaquin data, flow

conditions were constant throughout the deployment according to a downstream gauging station. Salinity conditions entering the confluence were relatively constant according to upstream gauging stations on both rivers. Furthermore, duplicate high resolution scans on Oct 6 and 7 yielded very similar SC distributions (see discussion below), suggesting that transport conditions were also constant during the course of a high resolution scan.

Both the Medea Creek and San Joaquin River NIMS RD scans yielded cross-sectional hydraulic and SC distributions at resolutions that would be difficult to obtain manually. The resulting monthly 24-hour scans at Medea Creek revealed previously unobserved spatiotemporal stream constituent patterns. For a given constituent, discernable, interrelated spatiotemporal patterns on several scales were observed. We focus on electrical conductivity (SC) and temperature (T) to illustrate these patterns and relationships. T and SC showed varying cross-sectional patterns throughout the 24-hour scan (examples in Figure 3). For both parameters, the patterns invert over the 24-hour period and seem related to the direction of the temporal patterns described below. To explore temporal patterns, the sample points in each cross-sectional scan were averaged and the average values plotted over time. Both T and SC displayed repeating sinusoidal diel fluctuations independent of the spatial variation (Figure 4a and Figure 5a). The sinusoidal pattern for T tracks expected air temperature patterns. The sinusoidal pattern for SC is the inverse of the T pattern and exhibits greater variability within the 24-hour period. Urban runoff pulses from lawn watering and other outdoor water usage may be a contributing factor to the greater variability of the SC pattern. Seasonal trends of increasing/decreasing amplitude and range of the temporal fluctuations were suggested for

both T and SC; however, additional monthly deployments will be needed to explore the consistency of these seasonal trends.

To investigate how the variation in the cross-section parameter values changed over time, the difference between the maximum and minimum value for each discrete cross section was calculated and plotted over the 24-hour period (Figure 4b and Figure 5b). The cross-sectional variation was consistently lower during the late nighttime and morning hours than during the afternoon and early nighttime hours. Although both SC and T showed the same general trend, the trend for T was more apparent.

All the aforementioned trends may be a product of any combination of urban influences, biological processes, and chemical processes. Although this observational study does not identify the mechanism(s) behind these trends, it does stimulate hypotheses and demonstrate the importance of considering small-scale spatiotemporal variation for stream monitoring and management. Without considering these spatiotemporal variations, a false conclusion about in-stream conditions could be made, which could lead to sub-optimal management practices.

The San Joaquin River low and high resolution velocity fields are plotted in Figure 6. As the contouring indicates, the low resolution field is characterized by some unrealistic patterns, while the higher granularity sampling effort seems to result in more natural patterns. Summary statistics for the two velocity fields are significantly different. The low resolution velocity scan resulted in maximum and mean velocities of 56.3 and 21.0 (SD 23.8) cm/s, respectively; the corresponding high resolution results are 60.6 and 36.4 (SD 19.2) cm/s for the Oct 6 scan, and 58.3 and 37.8 (SD 19.3) for the Oct 7 scan. The US Bureau of Reclamation Newman gauging station roughly 100 m downstream from the

NIMS RD cross-section indicated flow rates of 18.29 and 19.17 m^3/s, respectively (average values based on stage at the times of deployment). The total volumetric flow rate estimated by equation (1) for the low resolution scan was just 4.1% below this value (17.54 m^3/s), and the high resolution velocity distributions yielded a flows nearly the same as the gauging station values (18.38 m^3/s for Oct 6; 19.33 m^3/s for Oct 7).

High resolution SC scans for the San Joaquin River cross-section for Oct 6 and 7 are plotted in Figure 7. The maximum and mean SC values for the first scan were 1291 and 801 (SD 395) μS/cm, respectively; for the second scan these values were 1244 and 765 (SD 373) μS/cm. Given the lack of significant flow variation over this two-day period, the consistency of the SC distribution suggests that salinity inputs were relatively unchanged over the two-day period, and that the NIMS RD results are reproducible under steady flow conditions. It is worth noting that this point is true in spite of system dismantling and reassembly between the first and second scan (for security).

The total salt loads calculated by combining the information from the velocity and SC scans using equation (2) were 9.30 and 9.33 kg/s, respectively. The similarity of these numbers reinforces the reproducibility of the NIMS RD deployment method. Unfortunately, the downstream gauging station that was used to check the volumetric flow rate no longer records SC. However, these values are of the same order of magnitude as those estimated previously for this portion of the San Joaquin River (CDWR, 2003).

5. Conclusions

This paper introduces the NIMS RD technology for obtaining high resolution observations of spatiotemporal river channel hydraulic and water quality patterns. The

data available with the NIMS RD technology would be difficult to obtain in a reproducible manner using manually deployed sensors. The cases investigated here demonstrate that the system is suitable for small streams, yet structurally sound over spans exceeding 50 m. The Medea Creek case also demonstrates several successful autonomous deployments over periods exceeding 24 h. Results for Medea Creek temperature and SC clearly revealed spatiotemporal patterns that would be difficult to observe through continuous, single point monitoring. The San Joaquin River case demonstrated that the NIMS RD velocity distributions are in quantitative agreement with conventional flow-stage observations. Although analogous data were not available for validating the salt loads associated with SC distributions, the close agreement between the two scans suggests that NIMS RD can be used as a quantitative tool in evaluating distributed water quality properties and chemical fluxes in river systems.

References

Akima, H. (1978). A Method of Bivariate Interpolation and Smooth Surface Fitting for Irregularly Distributed Points. AMC Transactions on Mathematical Software. 4: 148-164.

Bachmayer, R. Leonard, N.E., Graver, J., Fiorelli, E., Bhatta, P., and Paley, D. (2004). Underwater Gliders: Recent Developments and Future Applications. *Proc. IEEE Int. Symp. Underwater Technol. (UT'04)*, Tapei, Taiwan.

CDWR (2003). *CalSim II Simulation of Historical SWP-CVP Operations*. California Department of Water Resources Technical Memorandum Report, 96 pp.

Doherty, K.W., Frye, D.E., Liberatore, S.P. and Toole, J.M. (1999). A Moored Profiling Instrument. *J. Atmos. Oceanic Technol*. 16 (11): 1816-1829.

Farrell, J.A., Pang, S. and Wei, L. (2005). Chemical Plume Tracing via an Autonomous Underwater Vehicle. *IEEE J. Oceanic Eng*. 30(2), 428-442.

Honji, H., Kaneko, A., and Kawatate, K. (1987). Self-Governing Profiling System. *Cont. Shelf Res*. 7(10), 1257-1265.

Kaiser, W., G. Pottie, M. Srivastava, G.S. Sukhatme, J. Villasenor, and D. Estrin(2004). Networked Infomechanical Systems (NIMS) for Ambient Intelligence in *Ambient Intelligence,* Springer-Verlag.

Laroche A.M., Gallichand J., Lagace R., Pesant A. (1996). Simulating atrazine transport with HSPF in an agricultural watershed. *J. Environ. Eng.-ASCE* 122 (7): 622-630.

Laval, B., Bird, J. S. and Helland, P.D. (2000). An Autonomous Underwater Vehicle for
the Study of Small Lakes. *J. Atmos. Oceanic Technol*. 17(1), 69-76.

Luettich, R.A., (1993). PSWIMS, A profiling instrument system for remote physical and
chemical measurements in shallow-water. *Estuaries*, 16(2): 190-197.

Ogren, P., Fiorelli, E. and Leonard N.E. (2004). Cooperative Control of Mobile Sensor
Networks: Adaptive Gradient Climbing in a Distributed Environment. *IEEE Trans.
Auto. Contr.*, Volume 49(8), 1292-1302.

Quinn, N.W.T., Jacobs, K., Chen, C.W. and Stringfellow W.T. (2005). Elements of a
decision support system for real-time management of dissolved oxygen in the San
Joaquin River Deep Water Ship Channel. *Environ. Modell. Softw*. 20(12), 1495-1504.

Reynolds-Fleming, J.V., Fleming JG, Luettich RA (2002). Portable autonomous vertical
profiler for estuarine applications**,** *Estuaries* 25(1), 142-147.

Walsh, C. J., Roy, A. H., Feminella, J. W., Cottingham, P.D., Groffman, P.M., Morgan,
R.P. (2005). The urban stream syndrome: current knowledge and the search for a cure.
J. N. Am. Benth. Soc. 24(3), 706-723.

Yu, X.R., Dickey, T., Bellingham, J., Manov, D. and Streitlien, K. (2002). The application
of autonomous underwater vehicles for interdisciplinary measurements in
Massachusetts and Cape Cod Bays. *Cont. Shelf Res*. 22(15), 2225-2245.
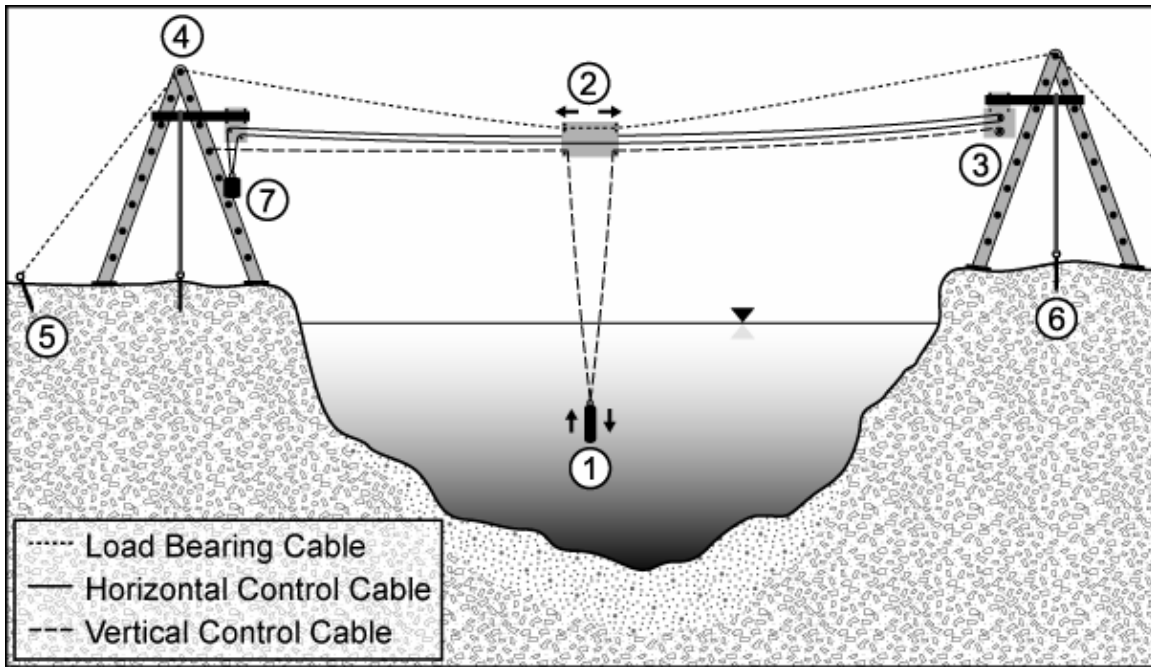
Figure 1. The NIMS RD system is shown in schematic view. The cableway system provides support for the sensor node payload (1). The cableway supports a horizontal actuator (2) controlled by an embedded computing system (3). The cableway is supported by aluminum support towers (4), and anchor systems (5), and (6), while a counterweight (7) provides tension.

Figure 2. Photographs of the NIMS RD Medea Creek 5m span deployment (top), and San Joaquin River 55m span deployment (bottom).
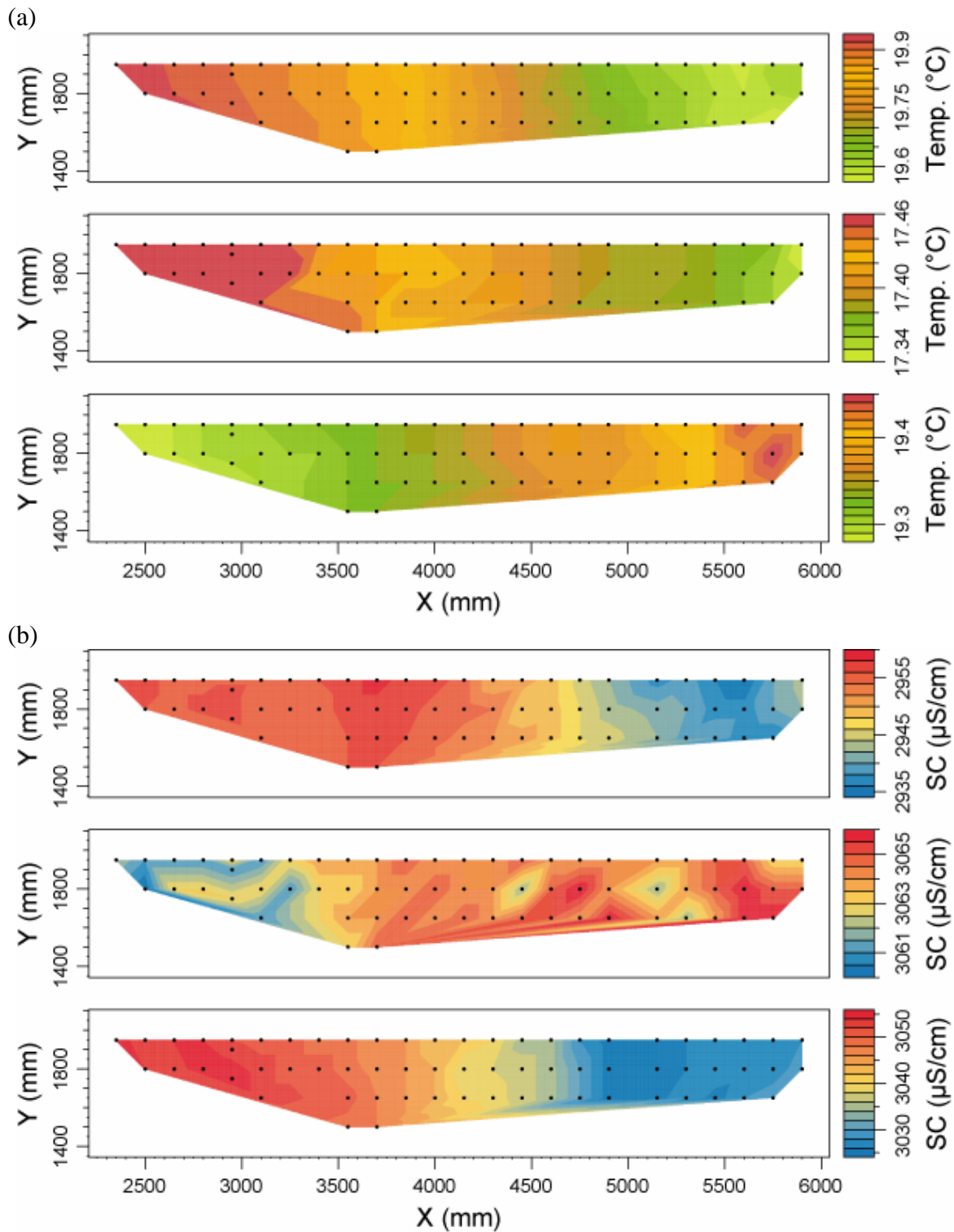
Figure 3. Typical cross-sectional (a) temperature and (b) specific conductance distributions produced during 24-h NIMS RD scans of Media Creek for Jul (top), Aug (mid), Sept (bot) 2005 (plot aspect ratio is 1:1).
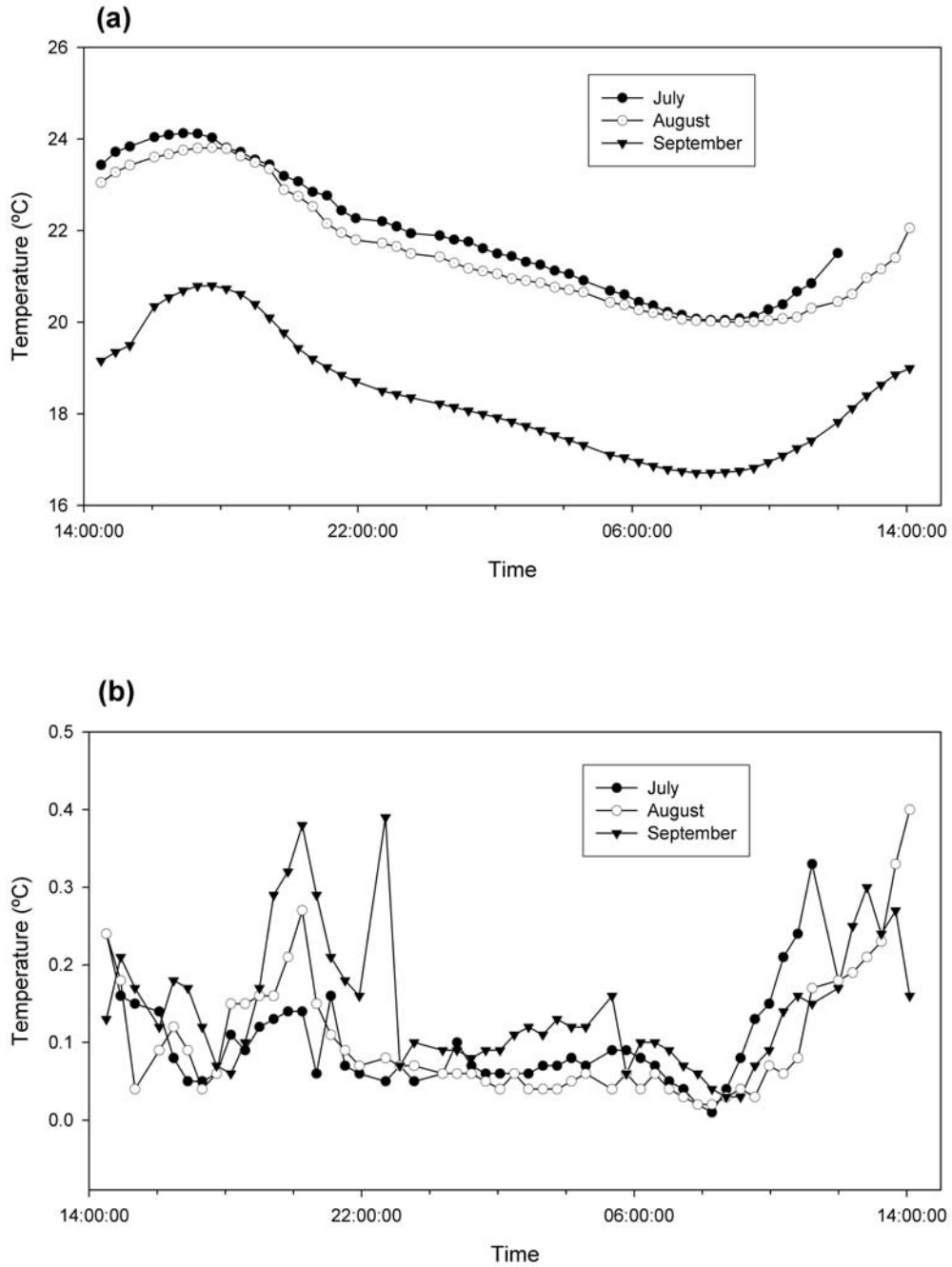
Figure 4. (a) Spatially averaged stream temperature variation over 24-hr periods in three different months; (b) variation in maximum temperature range ($T_{max} - T_{min}$) observed in cross-sectional NIMS RD scans (both for Jul, Aug, Sep Medea Creek NIMS RD deployments).
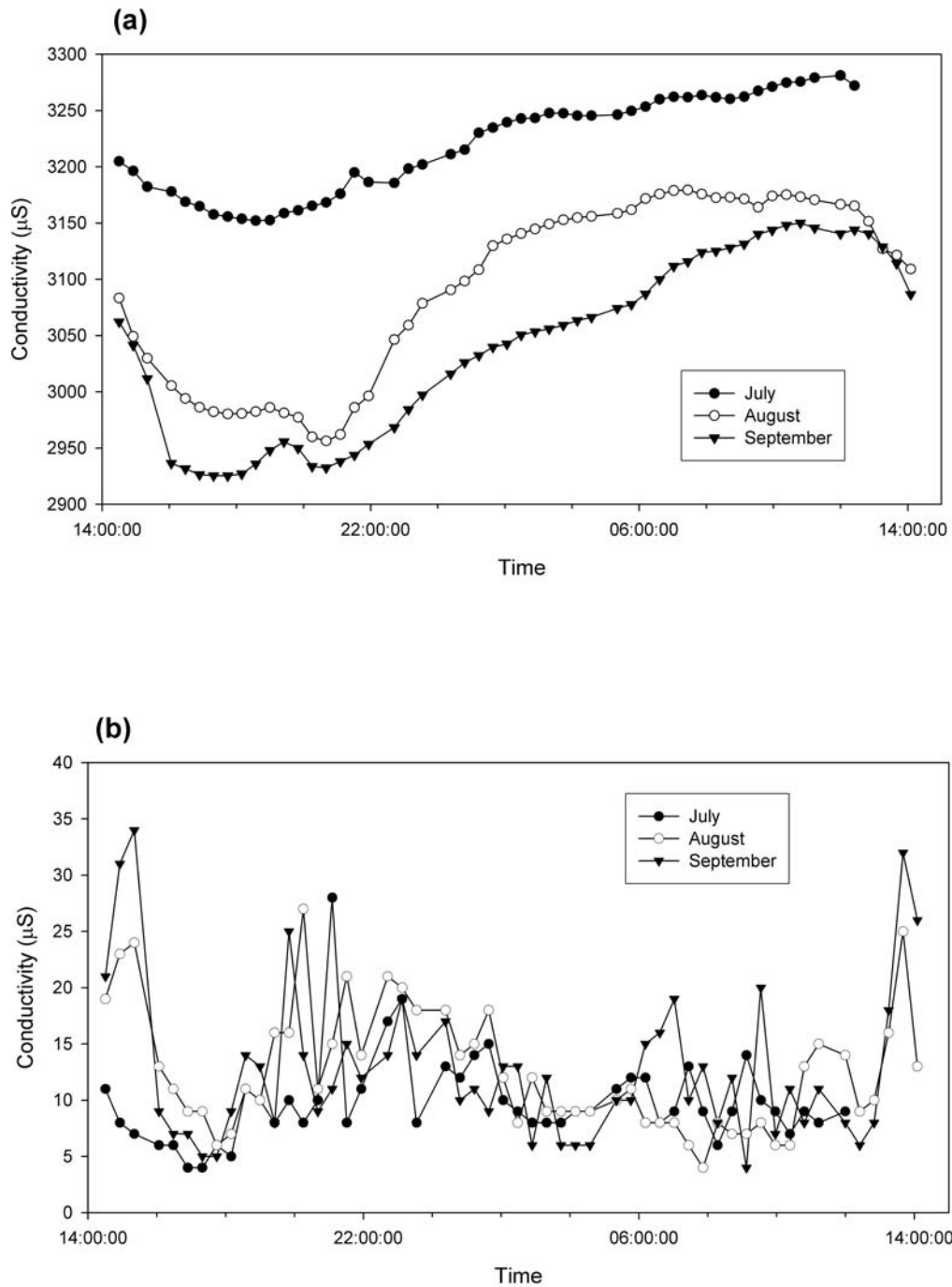
Figure 5. (a) Spatially averaged stream specific conductivity (SC) variation over 24-hr periods; (b) variation in maximum SC range ($SC_{max} - SC_{min}$) observed in cross-sectional NIMS RD scans (both for Jul, Aug, Sep Medea Creek NIMS RD deployments).
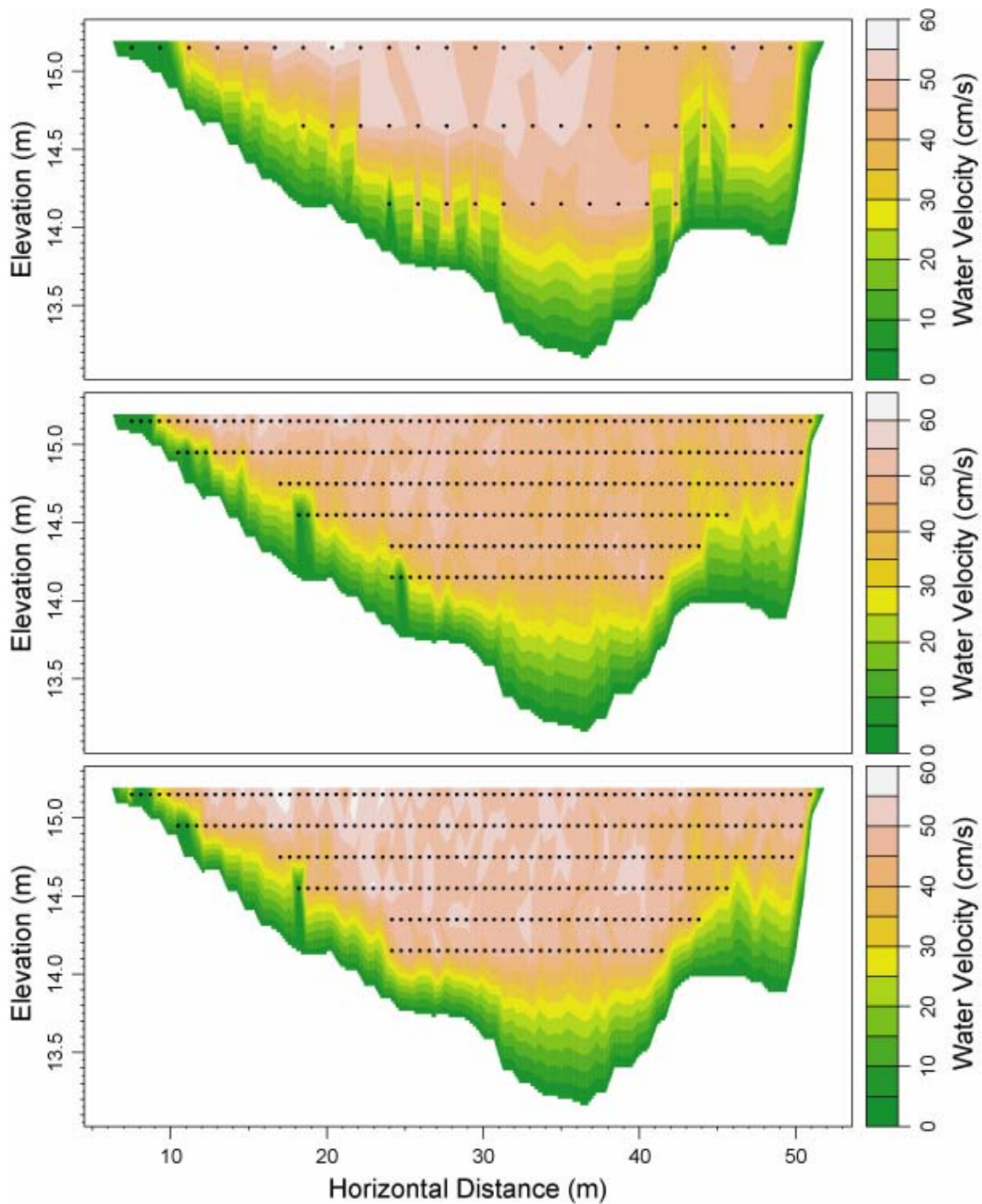
Figure 6. Low resolution (10/6/05 top) and high resolution (10/6/05 middle, 10/7/05 bottom) cross-sectional acoustic Doppler velocity (ADV) distributions generated during the San Joaquin River NIMS RD deployment (note: plot aspect ratio is 10:1).
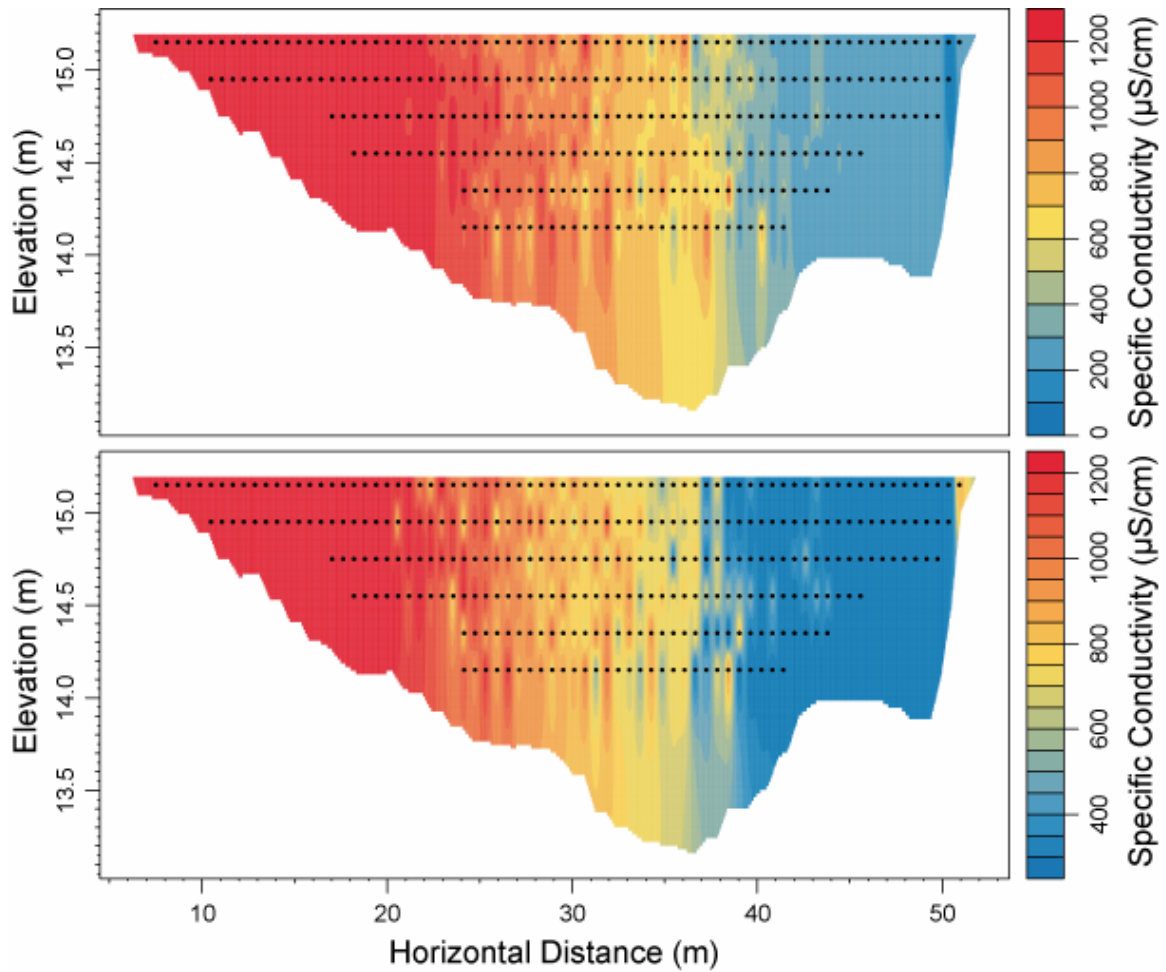
Figure 7. High resolution (10/6/05 top, 10/7/05 bottom) cross-sectional specific conductivity (SC) distributions generated during the San Joaquin River NIMS RD deployment (note: plot aspect ratio is 10:1).